

## X-Ray Emission Following Low-Energy Charge Exchange Collisions of Highly Charged Ions

P. Beiersdorfer,<sup>1</sup> R. E. Olson,<sup>2</sup> G. V. Brown,<sup>1</sup> H. Chen,<sup>1</sup> C. L. Harris,<sup>3</sup> P. A. Neill,<sup>3</sup> L. Schweikhard,<sup>4</sup>  
S. B. Utter,<sup>1</sup> and K. Widmann<sup>1</sup>

<sup>1</sup>*Department of Physics, Lawrence Livermore National Laboratory, Livermore, California 94550*

<sup>2</sup>*Department of Physics, University of Missouri-Rolla, Rolla, Missouri 65401*

<sup>3</sup>*Department of Physics, University of Nevada Reno, Reno, Nevada 89557*

<sup>4</sup>*Institut für Physik, Johannes Gutenberg-Universität, D-55099 Mainz, Germany*

(Received 12 July 2000)

*K*-shell x-ray emission following low-energy charge exchange collisions ( $\leq 11$  eV/amu) has been measured for ten bare and hydrogenic ions up to  $U^{91+}$ . The data resolve capture into angular momentum states with  $\ell = 1$  and provide a stringent test of theory. The assumption of Stark mixing of angular momentum states is inappropriate at such energies. Results from detailed calculations give a better description of the data, but significant discrepancies are noted. The measurements show that the hardness ratio of charge-exchange induced *K*-shell x-ray emission represents a diagnostic of the dynamics of ion-atom interactions in situations where the energy is below 1 keV/amu, e.g., in solar wind collisions.

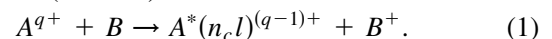
PACS numbers: 34.70.+e, 32.30.Rj, 32.70.Fw, 52.70.La

Charge exchange between ions and atoms or molecules strongly influences the ionization equilibrium of many laboratory plasmas and determines the ion storage time in ion traps and ion storage rings [1–4]. Charge exchange reactions were found to be crucial for understanding energy transport in the edge regions of magnetic fusion plasmas, and the associated energy loss may be the key for the success of radiative divertors in future reactor-type devices [5,6]. Spectral diagnostics in the visible and ultraviolet wavelength band based on charge exchange have become a method of choice for determining transport in beam-heated plasmas [7–9]. The recent discovery of x-ray emission from comets has focused new attention on charge exchange [10–12]. After some debate, charge exchange between solar wind heavy ions and cometary gases has emerged as the most likely mechanism for x-ray production, and efforts have been started to develop accurate descriptions of the process [13–15]. Very recently, charge exchange has also been implicated as a major contributor to the soft x-ray background of the heliosphere [16].

The low-energy conditions leading to cometary x-ray emission, determined by solar wind speeds ranging from 200 to 800 km/s outside the bow shock region to 100 km/s or less ( $\leq 50$  eV/amu) inside the bow shock region, stress aspects of charge exchange reactions not studied before. In fact, x-ray production following charge exchange itself has received very little theoretical or experimental attention. Knowledge of the total charge exchange cross sections combined with the assumption of statistical populations of angular momentum states, a procedure employed in high-energy charge exchange collisions, are not sufficient to describe the emission. Statistical assumptions, i.e., assumptions of Stark-level mixing, break down in low energy collisions, and proper description requires a detailed understanding of the angular momentum states formed during charge exchange [17,18].

In this Letter, we present measurements of the *K*-shell x-ray emission following low-energy charge exchange collisions involving highly charged ions. Our measurements extend from neon to uranium and allow us to infer the total angular momentum of the captured electron from the observed spectral emission. The measurements unequivocally demonstrate that statistical assumptions are not valid for describing low-energy collisions. Indeed, we find clear spectral signatures useful for determining the deviation from statistical equilibrium. These signatures represent an excellent spectral diagnostic tool for determining the collision properties of ion-atom interactions in a variety of natural phenomena, including x-ray emission from comets. Comparisons with detailed classical-trajectory Monte-Carlo (CTMC) calculations are presented and significant differences are uncovered that have yet to be understood.

Charge exchange is a process where an ion  $A^{q+}$  with charge  $q$  interacts with a neutral atom or molecule  $B$  by capturing one (or more) electrons:



The captured electron occupies a level with high principal quantum number  $n_c \approx q^{3/4}$ , where we ignore a slight dependence on the ionization potential of  $B$  [19]. The angular momentum  $\ell$  of the captured electron in high-energy collisions is described by statistics, so that the angular momentum state  $\ell = n_c - 1$  with a statistical weight of  $2\ell + 1$  has the highest likelihood of occupation. Statistical assumptions are not valid in low-energy collisions. This is because in the projectile's rest frame the angular momentum  $\ell$  carried by the electron due to the collision is given by the product of impact parameter  $b$  and the relative collision velocity  $v$  (in atomic units),

$$\ell = b \times v. \quad (2)$$

Approximating  $b$  by the square root of the charge exchange cross section  $\sigma$  divided by  $\pi$ , which roughly scales as

$\sigma \approx 16q$  [20], we get

$$\ell = (5q)^{1/2}v. \quad (3)$$

This argument predicts that the  $\ell = 1$  angular momentum state is very nonstatistically populated for collision energies below 500, 140, and 80 eV/amu for bare neon, krypton, and xenon, respectively.

The value of the angular momentum strongly determines the radiative decay paths of the captured electron. High angular momentum states deexcite along the Yrast chain, i.e., in steps of  $\Delta n = -1$  and  $\Delta \ell = -1$ , emitting a sequence of low-energy photons. The dominant  $K$ -shell x ray produced in this case is by decay from  $n = 2$  to  $n = 1$ . Direct decay from  $n = n_c$  to  $n = 1$  is very small and is given approximately by the fractional occupation of the  $n = n_c$ ,  $\ell = 1$  state ( $p$  state); i.e., the intensity ratio  $\mathcal{H}$  of  $n_c \rightarrow 1$  to  $2 \rightarrow 1$  decay in the high-energy limit is

$$\mathcal{H}_{\text{high-}E} \approx \frac{3}{\sum_{\ell=0, \ell \neq 1}^{n_c-1} (2\ell + 1)} \approx \frac{3}{n_c^2 - 3}. \quad (4)$$

Observation of  $K$ -shell x rays from  $n_c \rightarrow 1$  is, therefore, a measure of the population of low-angular momentum ( $p$ ) states. As the collision energy decreases, the fraction of electron capture into  $\ell = 1$  increases, and the hardness ratio  $\mathcal{H}$  of x rays from  $n_c \rightarrow 1$  to  $2 \rightarrow 1$  decays will increase accordingly.

Using the classical trajectory Monte Carlo (CTMC) method [21] and a radiative decay matrix valid for hydrogenic ions, we calculated the hardness ratio  $\mathcal{H}$  of x rays emitted by direct decay from  $n \rightarrow 1$  to  $K\alpha$  decay from  $2 \rightarrow 1$  as a function of collision energy. The results are shown in Fig. 1 for  $\text{Ar}^{17+}$  and  $\text{Xe}^{53+}$  ions. The figure shows that  $\mathcal{H}$  approaches the statistical value  $\mathcal{H}_{\text{high-}E}$  for collision energies above 1000 and 250 eV/amu for Ar and Xe, respectively. But the fraction of  $n_c \rightarrow 1$  emission is significantly enhanced at low collision energy, as an increasing number of electrons are captured into low angular momentum states.

Our measurements were carried out at both the high-energy Livermore electron beam ion trap, SuperEBIT, and low-energy electron beam ion trap, EBIT-II, making use of a new mode of operation introduced recently [22,23]. In this mode, dubbed the magnetic trapping mode, the electron beam is turned off after production of highly charged ions and EBIT is operated like a Penning trap. In the absence of the electron beam, the ions are confined on the order of seconds in the 3-T magnetic field generated by superconducting Helmholtz coils and the potential applied to the outer electrodes of the cylindrical trap. The trapping potential limits the energy of the ions, as ions with sufficient kinetic energy can overcome the potential barrier and leave the trap. The lower- $Z$  ions ( $Z \leq 36$ ) were confined with a 300-V barrier, the higher- $Z$  ions with a 150-V barrier, and U with a 10-V barrier. Based on earlier measurements [24], these conditions mean that the temperature of the ions ranges from  $10 \pm 4$  eV/amu for Ne, Ar, and Kr,

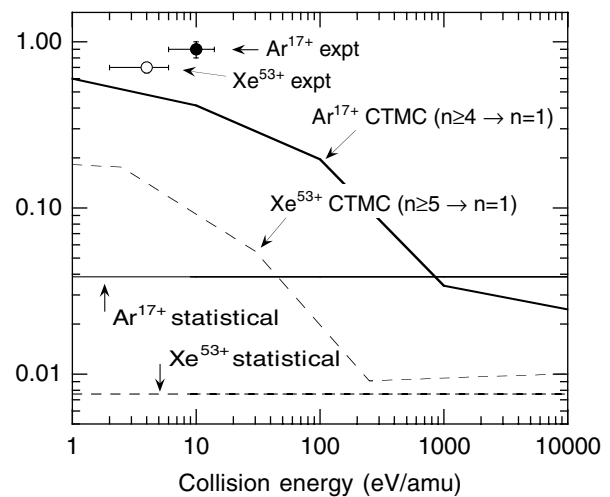


FIG. 1. Calculated ratio of  $n \rightarrow 1$  to  $2 \rightarrow 1$   $K$ -shell x-ray emission as a function of collision energy. Values shown are for  $\text{Ar}^{18+} + \text{H} \rightarrow \text{Ar}^{17+} + \text{H}^+$  and  $\text{Xe}^{54+} + \text{H} \rightarrow \text{Xe}^{53+} + \text{H}^+$ . Calculations employed the CTMC method and a hydrogenic radiative cascade matrix. Charge exchange partners other than atomic H do not significantly alter the results shown. Observed ratios are plotted as a solid circle for  $\text{Ar}^{18+}$  interacting with Ar and an open circle for  $\text{Xe}^{54+}$  interacting with Xe.

to  $4 \pm 2$  eV/amu for Xe and Au, and  $0.8 \pm 0.4$  eV/amu for U.

Because the ions are generated *in situ*, transfer losses are avoided and as many as  $10^7$  ions are available for study in the case of Ne and Ar, fewer for the higher- $Z$  ions. Only as few as 500  $\text{U}^{91+}$  ions and insignificant amounts of  $\text{U}^{92+}$  ions were generated in our trap during these measurements. Charge exchange was induced by ballistic injection of gases. The injector was operated either in a continuous mode [23] or in a pulsed mode [25]. X-ray spectra were recorded with a high-purity Ge detector, both before and after the beam was turned off, as illustrated in Fig. 2.

The charge-exchange-induced  $K$ -shell emission spectra from hydrogenic and heliumlike argon are shown in Fig. 3,

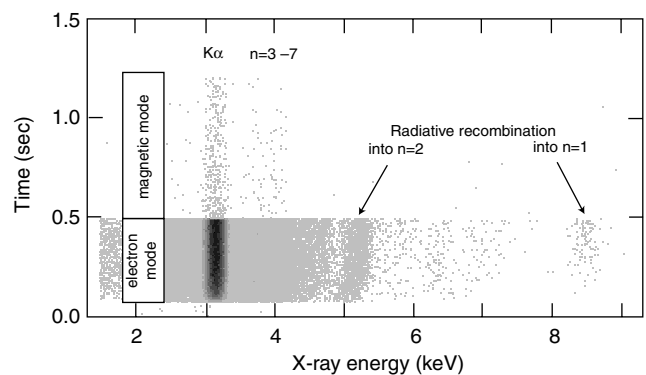


FIG. 2. Argon x-ray emission observed during the electron mode (beam on) and magnetic mode (beam off). Radiative capture of beam electrons during the electron mode results in prominent  $K$ -shell and  $L$ -shell emission from  $\text{Ar}^{16+}$  ions. The beam energy is 4.3 keV, i.e., below threshold to produce bare argon ions. In the magnetic mode all x-ray production mechanisms cease except charge exchange.

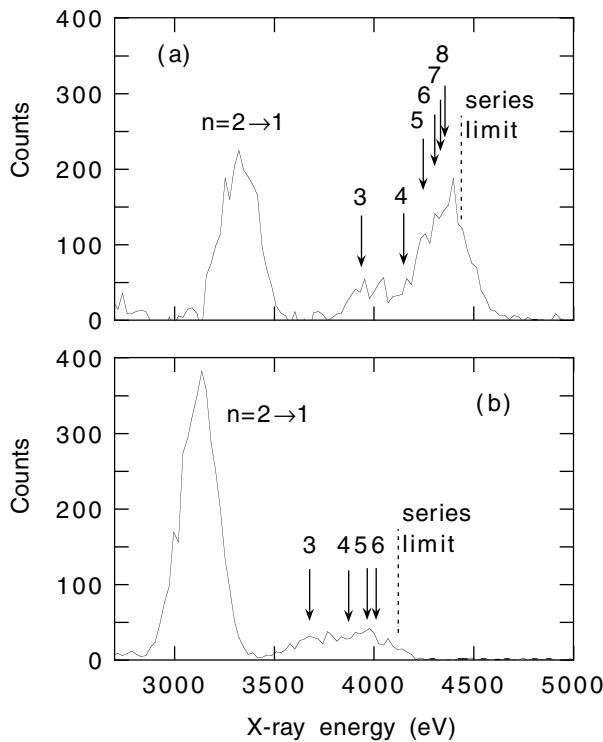


FIG. 3. *K*-shell emission spectra from hydrogenic and helium-like argon following the charge exchange reactions (a)  $\text{Ar}^{18+} + \text{Ar}$  and (b)  $\text{Ar}^{17+} + \text{Ar}$ . Emission emanating from different  $n$  levels is marked.

that from heliumlike gold in Fig. 4. While a pure spectrum of heliumlike argon can be generated by proper choice of the electron beam energy, the hydrogenic spectrum is admixed with heliumlike emission, which, however, can be subtracted out to yield the spectrum shown. From the spectra we can readily measure the ratio of  $n \geq 4 \rightarrow 1$  emission to  $2 \rightarrow 1$  emission. The ratio for  $\text{Ar}^{17+}$  is found to be  $30\times$  larger than predicted by statistical assumptions; the ratio of  $n \geq 5 \rightarrow 1$  emission to  $2 \rightarrow 1$  emission in  $\text{Xe}^{53+}$  is  $100\times$  larger (cf. Fig. 1). The measured values

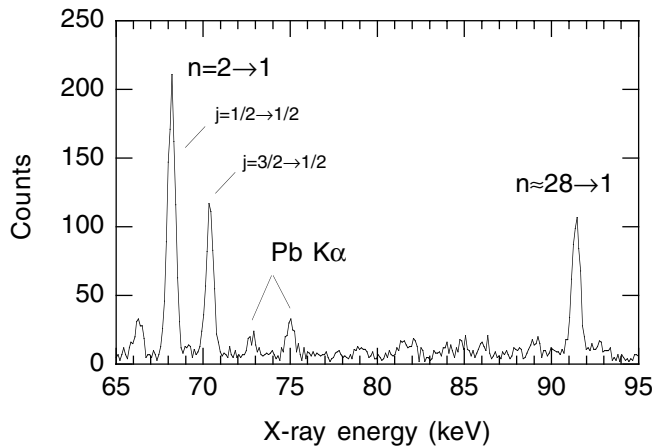


FIG. 4. *K*-shell emission spectra from heliumlike gold following the charge exchange reaction  $\text{Au}^{78+} + \text{Ne}$ . X rays of neutral lead are produced in the fluorescence of the shielding material surrounding the high-purity Ge detector.

of  $\mathcal{H}$  for all  $n \geq 3 \rightarrow 1$  x rays are shown as a function of  $Z$  in Fig. 5. The measured ratio from the hydrogenic ions is independent of  $Z$  and close to unity. In all cases, it is orders of magnitude higher than given by the assumption of Stark mixing, and significantly higher than the CTMC predictions.

The hardness ratio of high-to-low energy charge-exchange-induced *K*-shell emission from heliumlike ions is significantly lower than that for hydrogenic ions at low  $Z$  and rises with  $Z$ , as seen in Fig. 5. This rise is very different than predicted by statistics or CTMC calculations. To explain this phenomenon, we note that there is a coupling of the angular momentum between the  $1s$  electron in the initial hydrogenic ion and the electron captured during charge exchange. This coupling results in singlet and triplet states, which have very different radiative decay properties. For low- $Z$  ions, triplet states are spin forbidden to decay to the  $1s^2 \ ^1S_0$  ground level. A level of the type  $1sn_c p \ ^3P_1$  will decay instead to the  $1s2s \ ^3S_1$  level and only then via a magnetic dipole transition to the ground level. Direct *K*-shell emission from high- $n$  levels is, therefore, suppressed. As  $Z$  increases, spin-changing transitions become allowed, and the ratio of direct high- $n$  to  $2 \rightarrow 1$  emission increases, giving rise to an increase

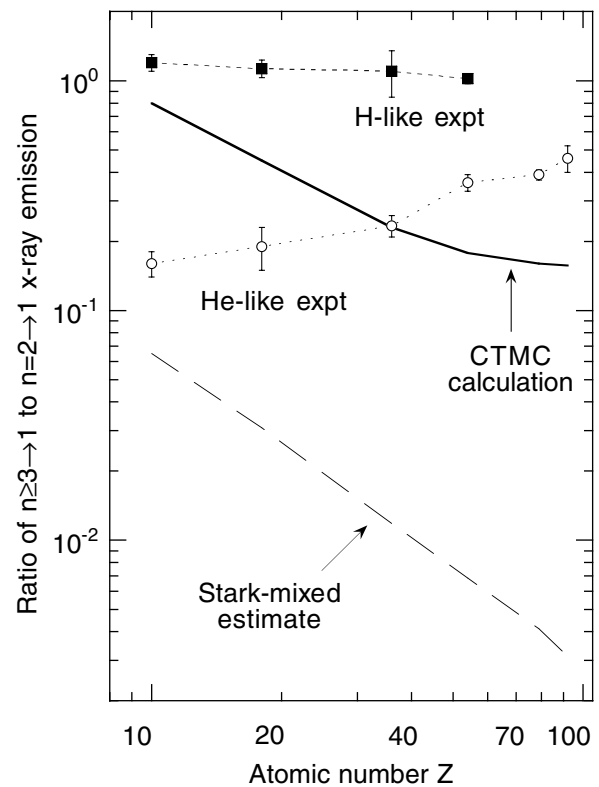


FIG. 5. Measured ratios of  $n \geq 3 \rightarrow 1$  to  $2 \rightarrow 1$  *K*-shell x rays from hydrogenic (solid squares) and heliumlike ions (open circles) as a function of atomic number  $Z$ . Results from CTMC calculations and estimates based on statistical populations of the angular momentum states are shown for comparison. The values for Ne, Ar, Kr, Xe, Au, and U were measured or calculated at collision energies of  $9 \pm 4$ ,  $10 \pm 4$ ,  $11 \pm 4$ ,  $4 \pm 2$ ,  $4 \pm 2$ , and  $0.8 \pm 0.4$  eV/amu, respectively.

seen in the data. Below xenon the measured values of  $\mathcal{H}$  are less than predicted by the CTMC calculations, above xenon they are larger. In all cases, however, the measured values by far exceed the statistical predictions.

In summary, the present observations provide a direct determination of capture into small angular momentum states and  $\ell = 1$  in particular, and thus a very detailed test of charge exchange theory at low collision energies not afforded by measurements of total capture cross sections or the values of  $n_c$ . The inferred fraction of capture into  $\ell = 1$  is not at all consistent with the assumption of Stark superposition, i.e., a statistical population of  $\ell$  values. Our measurements agree qualitatively with detailed CTMC predictions that show that low  $\ell$  values are preferentially populated at low collision energies. However, we find important differences: the fraction of  $K$ -shell emission from high- $n$  levels is substantially higher (up to factors of 2 at low  $Z$ , more at high  $Z$ ) than calculated. Such high emission levels from the  $\ell = 1$  state are predicted only for ion-atom collisions with a center-of-mass collision energy that is 1 to 2 orders of magnitude lower than is the case in our experiment (cf. Fig. 1). This indicates that the lowering of the angular momentum value sets in at a higher collision energy than predicted by the CTMC calculations. The calculations also do not account for multiple electron capture, which may play a role in the x-ray production; double capture was shown to be about 25% of single capture for highly charged xenon ions [3].

The fact that Stark mixing of angular momentum states is not a proper assumption for collision energies below a few keV/amu has profound effects on the spectral emission from many laboratory and astrophysical sources. For example, because  $n_c \rightarrow 1$  decay emits an x ray with energy about 25% higher than  $2 \rightarrow 1$  decay, the average x-ray energy and thus the hardness ratio increases. Optical and UV emission is suppressed, while the x-ray line emission is much more complex than predicted in the Stark-mixed case. Very importantly, the observed spectrum can be used as a diagnostic of the collision energy. Charge-exchange x-ray spectroscopy, even with moderate-resolution instrumentation, thus represents a new tool to determine the collision dynamics in a variety of natural phenomena, such as the slowing down of solar wind ions in cometary bow shocks or the heliopause, and thus can probe these interactions in novel ways.

This work was supported in part by the Office of Basic Energy Sciences of the U.S. Department of Energy and the Deutscher Akademischer Austausch Dienst and performed under the auspices of the Department of Energy by the University of California Lawrence Livermore National Laboratory under Contract No. W-7405-ENG-48.

---

[1] R. A. Hulse, Nucl. Technol. Fusion **3**, 259 (1983).

- [2] H. Geissel, K. Beckert, F. Bosch, H. Eickhoff, B. Franczak, B. Franzke, M. Jung, O. Klepper, R. Moshhammer, G. Munzenberg, F. Nickel, F. Nolden, U. Schaaf, C. Scheidenberger, P. Spädtke, M. Steck, K. Sümmerner, and A. Magel, Phys. Rev. Lett. **68**, 3412 (1992).
- [3] B. R. Beck, J. Steiger, G. Weinberg, D. A. Church, J. McDonald, and D. Schneider, Phys. Rev. Lett. **77**, 1735 (1996).
- [4] Th. Stöhlker, T. Ludziejewski, H. Reich, F. Bosch, R. W. Dunford, J. Eichler, B. Franzke, C. Kozhuharov, G. Menzel, P. H. Mokler, F. Nolden, P. Rymuza, Z. Stachura, M. Steck, P. Swiat, A. Warczak, and T. Winkler, Phys. Rev. A **58**, 2043 (1998).
- [5] W. P. West *et al.*, Plasma Phys. Controlled Fusion **39**, 295 (1997).
- [6] R. L. Boivin, J. A. Goetz, A. E. Hubbard, J. W. Hughes, I. H. Hutchinson, J. H. Irby, B. LaBombard, E. S. Marmor, D. Mossessian, C. S. Pitcher, J. L. Terry, B. A. Carreras, and L. W. Owen, Phys. Plasmas **7**, 1919 (2000).
- [7] R. J. Fonck and R. A. Hulse, Phys. Rev. Lett. **52**, 530 (1984).
- [8] R. C. Isler, Plasma Phys. Controlled Fusion **36**, 171 (1994).
- [9] E. J. Synakowski, R. E. Bell, R. V. Budny, C. E. Bush, P. C. Efthimion, B. Grek, D. W. Johnson, L. C. Johnson, B. LeBlanc, H. Park, A. T. Ramsey, and G. Taylor, Phys. Rev. Lett. **75**, 3689 (1995).
- [10] C. M. Lisse, K. Dennerl, J. Enghauser, M. Harden, F. E. Marshall, M. J. Mumma, R. Petre, J. P. Pye, M. J. Ricketts, J. Schmitt, J. Trümper, and R. G. West, Science **274**, 205 (1996).
- [11] K. Dennerl, J. Enghauser, and J. Trümper, Science **277**, 1625 (1997).
- [12] M. J. Mumma, V. A. Krasnopolsky, and M. J. Abbott, Astrophys. J. (Lett.) **491**, L125 (1997).
- [13] R. M. Häberli, T. I. Gombosi, D. L. De Zeeuw, M. R. Combi, and K. G. Powell, Science **276**, 939 (1997).
- [14] V. A. Krasnopolsky, Icarus **128**, 368 (1997).
- [15] R. Wegmann, H. U. Schmidt, C. M. Lisse, K. Dennerl, and J. Enghauser, Planet. Space Sci. **46**, 603 (1998).
- [16] T. E. Cravens, Astrophys. J. (Lett.) **532**, L153 (2000).
- [17] D. Dijkkamp, Yu. S. Gordeev, A. Brazuk, A. G. Drentje, and F. J. de Heer, J. Phys. B **18**, 737 (1985).
- [18] J. Burgdörfer, R. Morgenstern, and A. Niehaus, J. Phys. B **19**, L503 (1986).
- [19] R. E. Olson, Phys. Rev. A **24**, 1726 (1981).
- [20] R. E. Olson, K. H. Berkner, W. G. Graham, R. V. Pyle, A. S. Schlachter, and J. W. Stearns, Phys. Rev. Lett. **41**, 163 (1978).
- [21] R. E. Olson, J. Pascale, and R. Hoekstra, J. Phys. B **25**, 4241 (1992).
- [22] P. Beiersdorfer, B. Beck, St. Becker, and L. Schweikhard, Int. J. Mass Spectrom. Ion Process **157/158**, 149 (1996).
- [23] P. Beiersdorfer, L. Schweikhard, J. Crespo López-Urrutia, and K. Widmann, Rev. Sci. Instrum. **67**, 3818 (1996).
- [24] P. Beiersdorfer, A. L. Osterheld, V. Decaux, and K. Widmann, Phys. Rev. Lett. **77**, 5353 (1996).
- [25] L. Schweikhard, P. Beiersdorfer, G. V. Brown, J. R. Crespo López-Urrutia, S. B. Utter, and K. Widmann, Nucl. Instrum. Methods Phys. Res., Sect. B **142**, 245 (1998).